ELSEVIER

Contents lists available at ScienceDirect

Solar Energy

journal homepage: www.elsevier.com/locate/solener





Developments towards the heliostat field performance testing guideline[★]

Marc Röger ^{a,*} ^o, Tim Schlichting ^{b,1}, Jakob Herrmann ^{c,1}, Christoph Happich ^d, Daniel Nieffer ^{e,1}, Gerhard Weinrebe ^f ^o, Patrick Hilger ^g, Ansgar Macke ^{d,1}, Kristina Blume ^{b,1} ^o, Fabian Gross ^e ^o

- ^a German Aerospace Center (DLR), Institute of Solar Research, Calle Doctor Carracido 44, 04005 Almería, Spain
- ^b German Aerospace Center (DLR), Institute of Solar Research, Karl-Heinz-Beckurts-Straße 13, 52428 Jülich, Germany
- ^c Kraftanlagen Energies & Services GmbH, Ridlerstrasse 31c, 80339 Munich, Germany
- ^d CSP Services GmbH, Friedrich-Ebert-Ufer 30, 51143 Cologne, Germany
- ^e sbp sonne GmbH, Schwabstrasse 43, 70197 Stuttgart, Germany
- ^f Glasspoint Technology Center GmbH, Germany, previously sbp sonne GmbH, Germany
- g Synhelion Germany GmbH, Nikolaus-Otto-Straße 9, 52428 Jülich, Germany

ARTICLE INFO

Keywords: Concentrating solar power (CSP) Central receiver system Performance testing Quality assurance Heliostat Heliostat field Guideline

ABSTRACT

The final quality of each individual heliostat and its interaction as a heliostat field are important factors which determine the final performance and economic success of a solar tower system. The field quality is influenced by several factors like intelligent positioning of the individual heliostat units, their interaction (blocking/shading), light attenuation to the receiver, receiver optical acceptance angles, and operational parameters like calibration quality, aimpoint strategies, heliostat availability and reliability.

The Heliostat Field Acceptance Guideline is currently being developed to assess the quality of heliostat fields. This article gives background information and experiences which have been fed into the draft version of the new guideline for the heliostat field. The draft document will be shared with the community and will be a step forward in the measurement of distributed concentrator systems. It complements and builds on the existing SolarPACES Guideline for Heliostat Performance Testing, which allows the characterization of individual heliostats. The article discusses several options for heliostat field acceptance testing. The level-2 approach, based on statistical sampling of some heliostats and subsequent raytracing with measured and extrapolated values is recommended. The draft guideline also suggests various standardized tests and qualification procedures, providing an objective method to facilitate the field acceptance testing after construction, making it easier for suppliers and customers to negotiate contracts and ultimately reduce risks and costs.

1. Introduction

Standardization

In central receiver systems, hundreds to tens of thousands of heliostats are shaped to concentrate and biaxially track the sun onto a receiver that is located at the top of a tower. For high optical performance of the heliostat field, quality must be ensured at all relevant stages from design, manufacturing, commissioning and operation of the individual heliostat and the entire heliostat field. The heliostat field represents a significant portion, approximately 40 % to 50 %, depending on the specific boundary conditions, of the total capital cost of central receiver systems. Its performance is critical in providing the

concentrated solar radiation, essentially the "fuel" for the solar power plant. An acceptance test for industrial-sized heliostat fields should be available and agreed on to guarantee their high performance and reliability. That is, the annual or monthly amount of energy and/or the power at specific times of the year intercepted by the receiver aperture, should be measurable.

Flux measurement systems allows to measure incident power of concentrated solar radiation in or near the receiver aperture. The incident solar power together with other measurands allows to calculate either the solar field efficiency or the receiver efficiency. The efficiency of prototype receivers and tower systems are usually characterized by flux density measurement systems based on moving bars and

^{*} This article is part of a special issue entitled: 'Heliostats' published in Solar Energy.

^{*} Corresponding author at: German Aerospace Center (DLR), Institute of Solar Research, Calle Doctor Carracido 44, 04005 Almería, Spain. E-mail address: marc.roeger@dlr.de (M. Röger).

 $^{^{1}}$ Former.

Nomenclature		$N_{ m pop}$	Population size (all heliostats) (–)
		i	Heliostat number
Abbreviations		n	Sample size (chosen heliostats) (–)
BCS	Beam Characterization System	k	Rayleigh parameter, or coverage factor
CENER	Centro Nacional de Energías Renovables	P	Power (MW)
CSP	Concentrating Solar Power	$SD_{\mathrm{2D,RMS}}$	Root mean square value of 2D slope deviation matrix of
DBSCAN	Density-Based Spatial Clustering of Applications with		heliostat mirror surface (mrad)
	Noise	$Track_{2D,F}$	ICS,RMS Root mean square value of 2D tracking error (mrad)
DLR	Deutsches Zentrum für Luft- und Raumfahrt, German	V	Coefficient of variation $(=\sigma/\mu)$ $(-)$
	Aerospace Center	x	Heliostat field dimension, or parameter <i>x</i> (m)
D&S	Devices & Services Company	\overline{x}	Mean of parameter x
	Engineering, Procurement and Construction	у	Heliostat field dimension (m)
KDE	Kernel Density Estimation	z	Standard normal deviate (–)
	Heliostat Coordinate System		
	t Airborne Calibration Method for Heliostat Fields (DLR)	Greek syr	nbols
NIO	Non-Intrusive Optical Method (Sandia National	η	Efficiency (%)
	Laboratories)	μ	Mean value of a parameter (population)
	National Renewable Energy Laboratory	ξ	Mirror cleanliness (–)
	Reflected Target Non-Intrusive Assessment	ρ	Reflectance/reflectivity of clean mirror (%)
RMS	Root Mean Square	σ	Standard deviation of a parameter, orRayleigh parameter
	Sandia Optical Fringe Analysis Slope Tool		
	ES Concentrating Solar Power, Thermal and Chemical	Subscript	
bolaii i i G	Energy Systems – IEA Technology Collaboration	ap	aperture
	Programme	e	estimated
	Solar Tower Ray Tracing Laboratory, DLR	in	input
	Deflectometry Setup to Measure Heliostat Slope Deviation	field	field
~	Maps (CSP Services)	rec	receiver
	Typical Meteorological Year	S	sampled (parameter), or solar-weighted (reflectance)
1 1/1 1	Typical Meteorological Teal	sol	solar
English sy	mbols	th	thermal
$A_{ m net}$	Net heliostat aperture (m ²)	tot	total (solar to thermal)
	Error margin $(\overline{x} - \mu)$	λ	spectral, monochromatic
e*	Relative error margin $(=e/\mu)$ (%)	φ	acceptance angle, specular
-	Direct normal irradiance (W/m ²)		
∠ 0			

radiometers, e.g. [1–6]. In some experiments, the incident solar flux is estimated by raytracing simulations, e.g. [7].

Due to its size and cost, large-scale, industrial solar plants typically do not have moving bars or sufficient number of radiometers installed as usually found in protype receiver testing. Different R&D groups develop special flux measurement systems suited for large solar plants which are capable to measure the solar radiation which is directly reflected on the receiver surface [8–14]. Uncertainties between approximately 5 % and 6 % have been claimed; however, the number of validation experiments still seems scarce and more research in this direction is necessary.

For efficiency testing of the entire central receiver systems, i.e. the combination of solar field efficiency and receiver efficiency, please refer to the NREL report "Utility-Scale Power Tower Solar Systems: Performance Acceptance Test Guidelines" [15,16]. In this report, two tests are proposed which both include the receiver efficiency. The purpose of the power test is to measure the thermal power output under clear-sky conditions under thermal steady-state equilibrium conditions. The second test proposed by [15,16] is the multi-day continuous production test which validates the accuracy of the performance model for comparison to contractual projections.

The receiver efficiency as a separate part of the energy conversion chain can be determined without using solar flux measurement systems with tests developed during the Solar Two Project [17]. The power-on method eliminates incident power from the heat balance equation and calculates the thermal losses from known measurements. For this, the receiver is operated with 50 % and 100 % of the heliostat field around solar noon, while maintaining receiver outlet temperatures, that is heat losses, approximately constant. The power-off method circulates hot

fluid through the receiver while measuring the receiver heat loss without sun concentration on the receiver. The more flexible continuous power-on method [18] uses the ratio between arbitrary high and low incident power levels and can use more pairs than only the 50 % and 100 % level of the original Solar Two tests. Another method of [18] is the semi-analytical method which proposes to determine the heat loss by infrared camera readings of the receiver surface and the calculation the radiative and convective thermal losses. Xiao et al [19] present and validate a method which uses different direct normal irradiance conditions for the evaluation of thermal efficiency.

There is a gap in metrology for estimating the heliostat field efficiency as a separate part of the energy conversion chain. Heliostat field and receiver may be provided by different companies, so separate acceptance tests for heliostat field efficiency and receiver efficiency are necessary. The HelioCon roadmap [20] also indicates the necessity for in-situ monitoring tools for all opto-mechanical errors being applicable to commercial-scale heliostat fields. The SolarPACES grant "Analyze Heliostat Field" [21] supported the Heliostat Field Performance Testing Guideline activities by bringing together the world's metrology experts in measurement technologies of heliostats and heliostat fields to review, compare, and discuss the advantages and disadvantages of new and existing measurement methods.

For heliostat field efficiency testing, heliostat measurement techniques which allow to investigate a higher number of heliostats with low effort are required. There are techniques for quality assurance in manufacturing lines for single mirrors or the whole concentrator assembly, but also in-field techniques to characterize installed heliostats. One technology which can be found in practically all plants around the

world are beam characterization systems (BCS) [1,2]. They characterize the focal spot of one or several heliostats on a white target using a camera. This technology is usually used to measure the tracking accuracy. New developments additionally extract further information like slope error and focal length [22]. More recent developments even reconstruct the slope deviation maps solely from the flux images, either by using machine learning methods with prior training [23] or numerical optimization [24]. The BCS method using a white target suffers in large plants from contrast problems and not totally fitting heliostat focal spots on the physical target. CENER proposes a scanner-based methodology, a bar equipped with a vertical array of detectors and cameras, to characterize the focal spot and surface slope [25].

Mirror and concentrator shapes can be measured physically by deflectometry, e.g. the open source SOFAST [26,27], with its improvements regarding flexibility [28] and robustness [29], the QDec systems [30–32], the Bias-Fraunhofer deflectometry system [33], or the NREL ReTNA system [34,35] with reduced set up times regarding labor and infrastructure. Additionally, further developments in airborne in-field measurements techniques to measure slope deviation maps or tracking deviations, e.g. NIO [36,37], HelioPoint [38,39], or UFACET [40] may allow to go for an even more comprehensive qualification of installed heliostats including measurement of their orientation.

Mirror and concentrator shapes and its deformation with gravity can be measured by photogrammetry, e.g. [41]. Being limited in the past to measure heliostat shape and orientation from fixed or handheld cameras [42], nowadays cameras on drones can be used, see e.g. [43].

To fill the gap in determining the heliostat field efficiency, DLR, together with German industry, has initiated research with the final objective to develop a draft of a SolarPACES Heliostat Field Performance Testing Guideline. The project HELIODOR [44], funded by the German Federal Ministry for Economic Affairs and Energy, started in 2018 and ended in 2022. This paper presents final results of the project activities which have been used to draft the heliostat field guideline, lessons learned during the application of the guideline to a Juelich Solar Tower heliostat subfield and further insights.

The field guideline document will be made available for international review in the heliostat working group of SolarPACES Task III. It establishes different options for standardized test and qualification procedures each leading to comparable performance parameters for heliostat fields as an objective method for their efficient comparison. It should facilitate the acceptance testing after field construction, supports and speeds up the contract negotiations between heliostat field supplier and customer while lowering risks and costs. The guideline is directed to EPC contractors, field suppliers, third party testing companies, and plant owners. The guideline also offers templates for contracts and an exemplary acceptance procedure applied to a fictional 50-MW solar tower plant with 14,500 heliostats.

The SolarPACES Heliostat Field Performance Testing Guideline will complement the existing SolarPACES Guideline for Heliostat Performance Testing [45] which defines the parameters and respective measurement techniques for single heliostats. More information can be also found in the conference articles with updates [46,47], or the article describing the testing of the Stellio heliostat according to the guideline [48].

2. Requirements of heliostat fields

Besides the individual heliostat performance, the positioning of the heliostats and its interaction and operation as a unified field determine its quality and performance. The field design, manufacturing, commissioning, operation and maintenance should adhere at least to the following requirements:

 The heliostat field design must consider concentrator focal lengths, blocking/shading characteristics, light attenuation to the receiver, tower height, and receiver optical acceptance angles.

- The manufacturing process may involve either on-site assembly of structures and mounting of mirrors in local workshops or maximum prefabrication and transportation for minimal final assembly on-site.
 Quality control during manufacturing and after their transport to the final field location is essential.
- The final commissioned quality of the heliostat field, including optical and tracking accuracy and correct positioning, should ensure the contractually agreed energy production.
- Operational aspects require easy calibration, effective communication, and a high availability and reliability to maintain acceptable solar field performance.
- Low costs for production, installation, operation and dismantling.
- Speed of production and commissioning.
- Low environmental impact (e.g. reduced use of critical materials and chemicals, use of recyclable materials, low impact on soil and vegetation, low water usage, low energy consumption etc.).

3. Methodology

The drafted SolarPACES Heliostat Field Acceptance Guideline defines heliostat field interfaces, relevant field parameters and offers different approaches for acceptance testing. It also includes additional material, such as an exemplary acceptance procedure for a fictitious power plant, or a sample contract between the heliostat field manufacturer and the owner.

3.1. Definitions

The heliostat field has interfaces to the receiver, atmosphere, ground, the field power supply and global signal interface, see Fig. 1. The heliostat field control system including aim point strategies could be either part of the heliostat field, if it is delivered by the heliostat field manufacturer, or not, if delivered by others. The chosen option must be clearly defined in the contractual documents.

Relevant parameters of the heliostat field can be divided in the following subgroups:

- Performance Parameters: These parameters describe the technical properties of the whole heliostat field which determine the output of the power plant, e.g. the heliostat field efficiency, heliostat parameters (heliostat coordinates and orientation, heliostat geometry like reflective area, shape and kinematics, slope deviation, tracking deviation, reflectance), availability, energy consumption, time limits (startup, change of aimpoint etc.), and operational limits like wind and temperature.
- Communication and Safety Parameters: Although having minor effect on the electric output of the power plant, these parameters have to be fulfilled to ensure the safety of personnel and to prevent damages to equipment, e.g. flux limits, communication or power loss, reaction time, human/operational control failures, emergency measures, etc.
- Commercial Parameters: These parameters are commercially relevant for the project, e.g. capital costs, operating costs, maintenance/repair costs, cleaning costs, lifetime, degradation, required standards guidelines and local regulations.
- Environmental Parameters: The environmental parameters define the interfaces of the heliostat field to the atmosphere and ground in sufficient quality in spatial and temporal relation. The plant must be able to operate and survive under these environmental boundary conditions and provide the energy yield as indicated by simulations with a virtual heliostat field model using the same data. Weather data of a Typical Meteorological Year (TMY) may be used, together with other factors like long-term hail and snow, lightning, precipitation, wind events, corrosivity classification or time series of cleanliness, attenuation, soiling, etc.

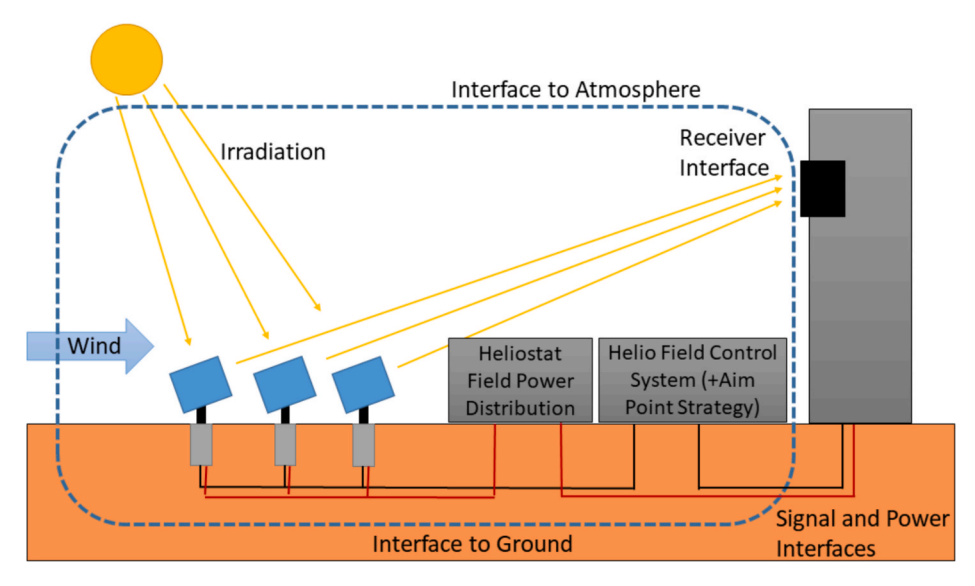


Fig. 1. Definition of the interfaces of the heliostat field to receiver, atmosphere, ground, field power supply and global signal network.

The parameters can be measured or estimated using different methods, with each parameter assigned to a specific category of method:

- Acceptance Tests: Parameters determined during the acceptance procedure at a specific point in time, usually after completion of the construction phase and during commissioning of the solar field. This means that these parameters result from the actual acceptance process on site.
- Time Evaluation: Parameters that cannot be tested in a single acceptance procedure, but must be evaluated over a period of time, e. g. the heliostat availability. Multiple measurements must be taken at intervals, or operational field data must be evaluated.
- Component Pre-Test: Not every component or element can be tested in the field during the acceptance procedure, e.g. the lifetime of components, or the mirror reflectance with spectrophotometers. They must be measured in the laboratory before shipment and not during manufacturing, to distinguish them from the on-site manufacturing quality control group. All warranties or guarantees of components are usually included in this label. It is necessary that the same batches, whose quality has been checked, are used for the heliostat field.
- On-site Manufacturing Quality Control: Results from on-site quality control systems, such as in-line slope deviation measurement, can be used for heliostat field acceptance. It is important to consider the potential impact of transport and final assembly at the destination in the solar field, for example by demonstrating with some sample measurements that there is no change in parameters due to transport in the field.
- Mathematical Proof: The parameters in this category cannot be measured directly, e.g. the annual energy output of the solar field in MWh, but their fulfilment is a decisive factor in determining whether or not an approval is granted. Therefore, a mathematical proof with further calculation steps based on measurements or component specifications is provided to meet this requirement. The simulationbased acceptance procedure falls into this category.

3.2. Phases of heliostat field performance testing

The drafted guideline provides an overview of the various phases involved in the process, from the initial contract negotiations through the installations of the first heliostats to the final commissioning of the entire field. This encompasses a range of activities, including the first batch check, heliostat field layout check, provisional acceptance, and

the final acceptance test, see Fig. 2.

In all cases, the overall acceptance procedure as well as all relevant parameters and quality criteria should be defined by the involved parties. It is recommended that the schedule is incorporated into the contract as an agreed-upon term. Fig. 3 illustrates the activities which should be completed in order to achieve final acceptance.

3.3. Performance testing using sampling

Different approaches are possible for the heliostat field acceptance testing. Wherever feasible, a 100 % qualification of all heliostats or heliostat components is recommended to ensure manufacturing and assembly quality. Commercially available in-line qualification tools for single mirrors or whole concentrators, or for already installed heliostats can be used for this task. Different R&D laboratories have prepared and partially commercialized via spin-off companies quality assurance solutions which cover the whole production chain from manufacturing (mirrors, concentrators) down to the installed single heliostat or whole heliostat field [21-35,41,42]. Additionally, further developments in airborne in-field measurements techniques to measure slope deviation maps or tracking deviations may allow to go for an even more comprehensive qualification of installed heliostats including measurement of their orientation, e.g. [36-40,43]. Where a 100 % qualification is not practical or feasible, measurements on a representative, statistically selected sample of heliostats can be performed. The measurement methods proposed by the (single) Heliostat Performance Testing Guideline [45] can be used.

3.3.1. Normally distributed populations

For the sampling, the HELIODOR project proposes at first a simple form of sampling: If the investigated parameter x is normally distributed, the population can be described with the mean value μ and the standard deviation σ .

Distribution function of the error of the mean of the population (central limit theorem).

The normalized distribution function of the mean value \overline{x} of a sample converges to a standard normal distribution with sufficient number of samples. This is true even if the parameter x itself is not normally distributed. The central limit theorem states that for a statistical sample of size n, with n approaching infinity, the random variable $\sqrt{n}(\overline{x}-\mu_{\overline{x}})$ converges to a normal distribution. With $\mu_{\overline{x}}=\mu_x=\mu$, one can also simpler write that $\sqrt{n}(\overline{x}-\mu)$ converges to a normal distribution. The normal distribution can be formulated by the standard normal deviate z.

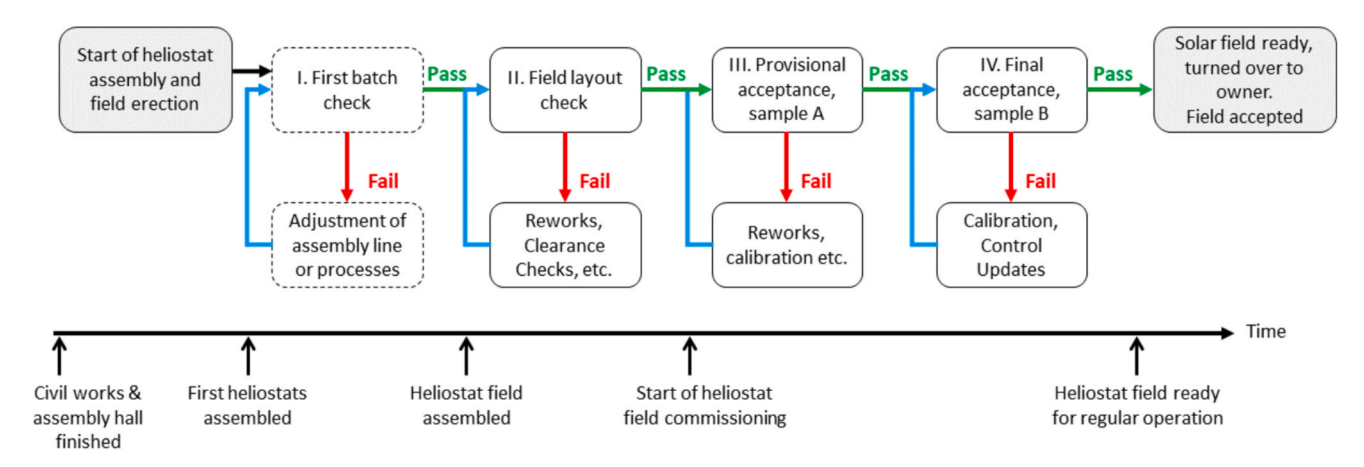


Fig. 2. Recommended workflow for quality assurance including heliostat field acceptance procedure.

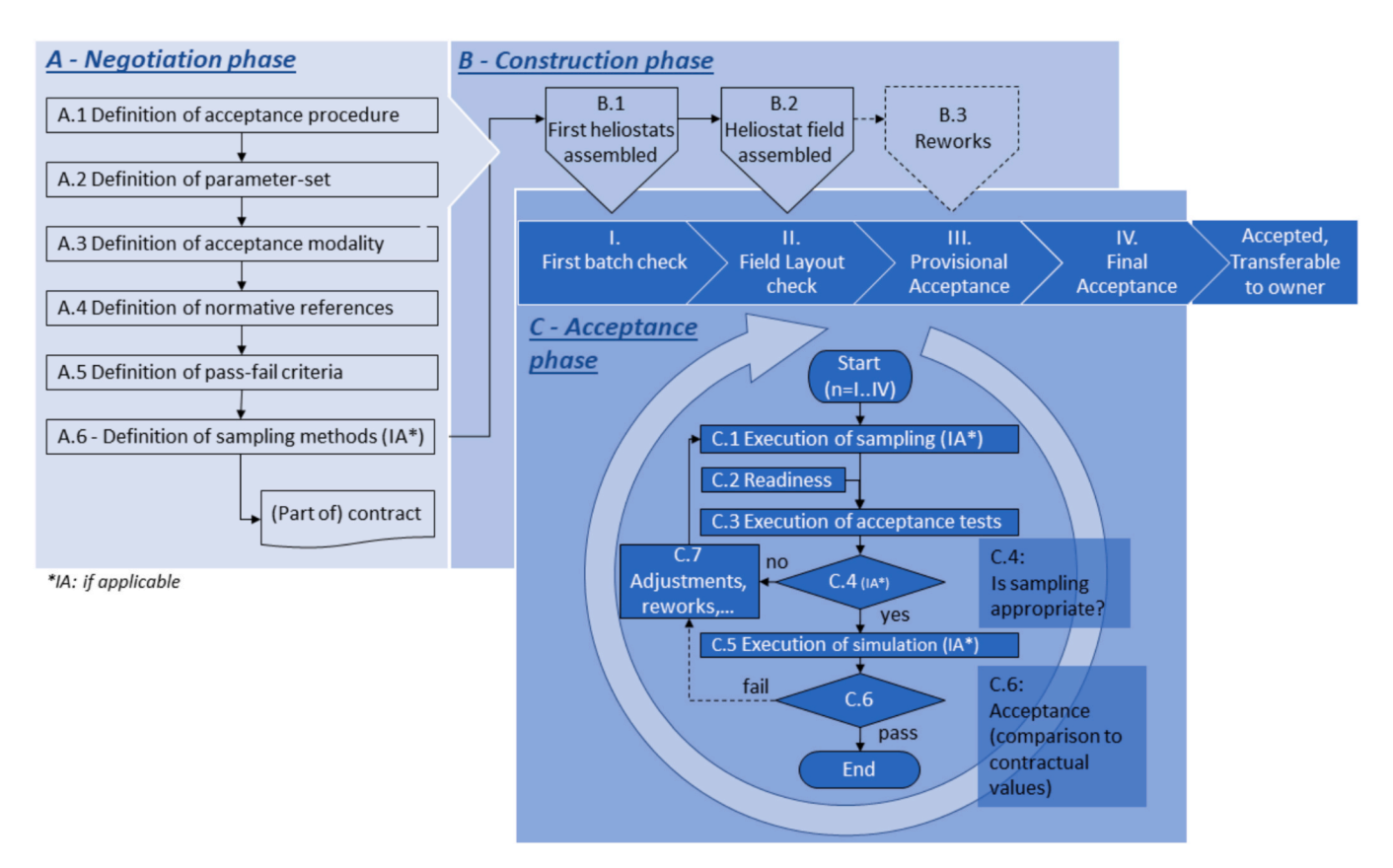


Fig. 3. Flow chart of recommended phases and their corresponding activities. The circular process shown within "C-Acceptance phase" is repeated for each stage I through IV.

Following this, the mean value \overline{x} of a parameter can be described by the mean value μ of the population and the standard deviation of the mean value $\sigma_{\overline{x}}$:

$$\overline{x} = \mu + \sigma_{\overline{x}} \bullet z = \mu + \frac{\sigma}{\sqrt{n}} \bullet z \tag{1}$$

The error value *e* can be defined as:

$$e = \overline{x} - \mu \tag{2}$$

It is the interval around a found sample mean value \overline{x} , within which the true mean value μ of the population is located with a certain probability described by the value z. Also, we can define a relative error $e^*=e/\mu$ with μ being the estimated mean value (μ _e) of the population. For example, if

a relative error e^* of \pm 5 % chosen, it is ensured that the sample mean value is found within the \pm 5 % of the true mean μ of the heliostat field.

With the definition of e and solving for n, the minimum statistical sample size of heliostats to be measured calculates to:

$$n = \frac{z^2 \sigma^2}{\rho^2} \tag{3}$$

The coefficient of variation V must be estimated. The estimated coefficient $V_{\rm e}$ is the ratio between the estimated standard deviation $\sigma_{\rm e}$ and the estimated mean value $\mu_{\rm e}$. The relative error margin is defined as $e^*=e/\mu_e$. Then, Eq. (3) can be also written in the form:

$$n = \frac{z^2 V^2}{e^{z_2}} \tag{4}$$

Since the number of heliostats in a field is not infinite, we can consider the mode 'pull without putting back', i.e. in total we have to get fewer samples. For a finite number of heliostats N_{pop} we can write, see also [49].

$$\overline{x} = \mu + \frac{\sigma}{\sqrt{n}} \sqrt{\frac{N_{\text{pop}} - n}{N_{\text{pop}} - 1}} \bullet z \tag{5}$$

Including e and solving for n results in the minimum statistical sample size in this case:

$$n = \left(\frac{z^2 \sigma^2}{e^2}\right) / \left(\left(1 - 1/N_{\text{pop}}\right) + \left(\frac{z^2 \sigma^2}{e^2 \bullet N_{\text{pop}}}\right)\right)$$
 (6)

or written with the coefficient of variation V and the relative error e^* :

$$n = \left(\frac{z^2 V^2}{e^{*2}}\right) / \left(\left(1 - 1/N_{\text{pop}}\right) + \left(\frac{z^2 V^2}{e^{*2} \cdot N_{\text{pop}}}\right)\right) \tag{7}$$

We observe that for large heliostat fields with high population size $N_{\rm pop}$, the term in Eq. (5) under the square root ($N_{\rm pop}$ -n)/($N_{\rm pop}$ -1) approximates one. Eq. (6) transforms to Eq. (3), and Eq. (7) transforms to Eq. (4). For medium and larger fields with $N_{\rm pop} > 100$, the term $(1-1/N_{\rm pop})$ in Eq. (7), approximates one. So Eq. (7) can be approximated also by the following form, sometimes called Slovin's formula:

$$n = \left(\frac{z^2 V^2}{e^{*2}}\right) / \left(1 + \left(\frac{z^2 V^2}{e^{*2} \bullet N_{pop}}\right)\right)$$
(8)

In short, if the heliostat property can be approximated by a normal distribution, Eq. (7) can always be used, the simplified Eq. (8) only for fields with more than 100 heliostats. Eq. (4) provides higher sample numbers, especially for smaller fields, so its use is always possible but not necessary.

3.3.2. Not normally distributed populations

The assumption of a normal distribution (Fig. 4 left) is not necessarily true for all parameters and the whole heliostat field. Examples are the distributions of the 2D slope deviation or the 2D tracking deviation. If optical errors around the single dimensions (x, y) are normally distributed errors, the convolution in two dimensions frequently results in a Weibull-type distribution (Fig. 4 middle).

Another example for a not normally distributed population is a heliostat field which has been constructed in several phases and the first sector might have resulted in worse quality. This would result in a distribution with two peaks which in some cases can be approximated by an overlay of two normal distributions each with different mean values and standard deviations (Fig. 4 right).

In these cases, the field cannot be represented by a simple mean value and the corresponding standard deviation, and the distribution function found has to be considered for performance testing.

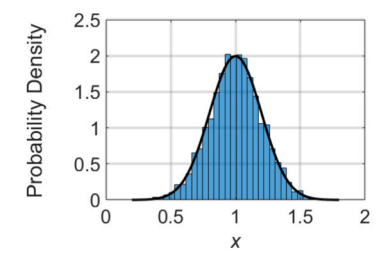
3.4. Approaches for performance testing

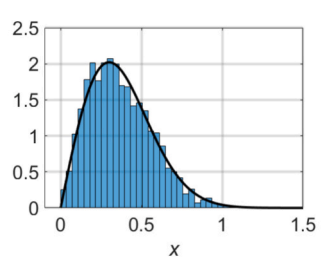
3.4.1. Level-1 approach: Heliostat properties only

The guideline allows different acceptance approaches for the

Table 1The different approaches of performance acceptance testing. Level 2 needs data from level 1. (* means within confidence interval).

	Heliostat properties only (level 1)	Simulation-based output (level 2)	Other Approaches
Acceptance Procedure	Define sampling method and measure individual heliostats of the sample	Define sampling and measure individual heliostats. Level 2: Data analysis (Anomalies), data extrapolation on unmeasured heliostats and raytracing yield simulation.	Define a measurement method to be used to derive solar field efficiency: - Solar flux measurement, or - Measurement of total efficiency and the thermal receiver efficiency.
Contract	Measured heliostat parameters (e.g. distributions of permitted tracking deviation, stope deviation, etc.) comply with* the contractual design values?	Simulation-based heliostat field efficiency, or heliostat field yield (yearly/monthly/ daily MWh) comply with* the contractual design value?	Heliostat field efficiency, or input power into receiver at certain operating conditions comply with* with the contractual design value?
Complexity for companies or R&D institutions with expertise on heliostat metrology	Moderate	Moderate, but additional steps for raytracing compared to level 1 is needed (raytracing software incl. all input data)	Moderate
Uncertainty of field performance	Depends on sample size	Uncertainty ~ 3 % (with sufficient sample size and validated raytracing software)	Medium-high, depends on future R&D
Limitations	Not considered are: • Field layout effects and • Aimpoint strategies	Aimpoint strategy, as defined in the contract, is considered. Raytracing software must be validated and same software for contract and acceptance calculations must be used. Recommended approach.	Requires flux measurement system with high accuracy, or receiver efficiency measurement with lower uncertainties than state-of-the-art. Depends on actual operating conditions.





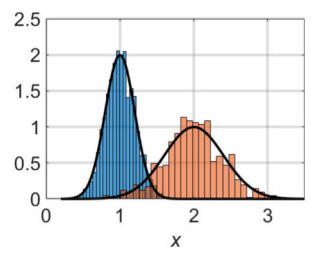


Fig. 4. Schematic of three prototype distributions: Normal distribution (left; μ =1.0 mrad, σ = 0.2 mrad), Weibull-type distribution (middle; as Rayleigh distribution k=2; $\lambda=\sigma=0.42$ mrad) and overlay of two normal distributions (right; $\mu_1=1.0$ mrad, $\sigma_1=0.2$ mrad, and $\mu_2=2.0$ mrad, $\sigma_2=0.4$ mrad)).

heliostat field acceptance testing, see also Table 1. The level-1 approach only compares individual heliostat characteristics (e.g. slope deviation, tracking deviation, etc.) as defined in the Guideline for Heliostat Performance Testing [45–47] after selecting a statistically relevant number of heliostat samples. It then compares every measured quantity, e.g. distributions of permitted tracking deviation, slope deviation, etc., with the respective contractually agreed values and returns a pass or fail output.

3.4.2. Level-2 approach: Simulation-based output

The level 2 approach uses either the heliostat field efficiency or heliostat field yield in MWh, expressed as yearly, monthly or daily mean efficiency values or integral yield data for a year, months, or days using a predefined Typical Meteorological Year. It builds upon the results of the level-1 approach, because the performance parameters obtained from individual heliostats investigated in level 1, serve as inputs for constructing a virtual representation of the solar field in a raytracing software. Modern raytracing software can assign individual values to each heliostat. These values with their found spatial distribution over the field, like local anomalies or clusters, can be used instead of mean values and standard deviations.

In the following, four steps are shortly explained: (1) Data exploration and cluster analysis, (2) Resampling, (3) Data extrapolation, (4) Data assignment and raytracing.

- (1) Data Exploration and cluster analysis. After measuring the performance parameters of selected heliostat samples, the resulting dataset undergoes a data exploration to identify local anomalies or clusters. A density-based clustering approach, for example the DBSCAN algorithm can be applied using each heliostat's geospatial position with a performance parameter, for example the slope deviation. DBSCAN automatically groups points which are closely packed together and flags outliers that deviate significantly from their neighbors. This is ideal for spotting local anomalies or clusters in the heliostat field.
- (2) Resampling. In cases where local anomalies or clusters of significantly higher or lower values appear, the level-2 approach is preferred and additional samples are collected from those specific regions to validate findings and refine the analysis. The resampling is performed independently for each performance parameter, ensuring that each parameter (e.g., slope deviation, reflectance) receives an individual examination. Re-running the clustering with the new data lies the basis for the level-2 analysis, which provides a deeper understanding of emerging patterns and helps to confirm or refute initial observations. The procedure of data sampling and refinement is described in the draft guideline document and is explained in detail in a separate scientific article [50] focusing on statistics and cluster analysis. By combining position and performance in the clustering process, local clusters of abnormal or especially high-performing heliostats can be detected, guiding either targeted improvements, maintenance or further investigation.
- (3) Data Extrapolation. The results of the measured heliostat individuals are extrapolated to unmeasured heliostats for the raytracing simulation. The distribution function for each sampled performance parameter (e.g. slope deviation) is aligned with the unknown distribution function characterizing the entire heliostat field or field clusters to generate synthetic data for the unsampled heliostats. It is crucial that the distribution function remains unaltered throughout the synthetic data generation process. This can be achieved by using a kernel density estimation technique (KDE). KDE is a nonparametric method that avoids making assumptions about the data's underlying shape. Instead of forcing the data into a particular distribution, like e.g. a normal or gamma distribution, KDE constructs a smooth probability density function. It places small often Gaussian-shaped "kernels" around each observed data point and summarizes these kernel functions. This approach ensures that important features of the sampled distribution, such as skewness, multiple peaks, or heavy tails, are accurately captured and preserved. KDE solves the problem of smoothing data by allowing a

limited sample to be used to infer a population. Once the KDE is formed, synthetic data can be drawn from this estimated density, guaranteeing that the statistical properties remain consistent with those in the original heliostat measurements. Prior resampling increases the information amount for the estimation technique.

(4) Data Assignment and Raytracing. The virtual heliostat field is created by assigning performance parameters to unmeasured individuals in accordance with the distributions of the identified local anomalies and clusters. The resulting virtual heliostat field model allows for the calculation of hourly or annual efficiencies for the entire manufactured heliostat field. Modern raytracing simulation tools which have been validated against beam characterization measurements must be used for this calculation, and the same raytracing software must be used during contract negotiations and acceptance testing to avoid any differences caused by different software implementations. Raytracing calculations can be compared against in-situ flux measurements obtained from individual heliostats or groups to validate the simulated power outputs during the acceptance test.

3.4.3. Other approaches

Further measurement methodologies for assessing the heliostat field efficiency are either (1) solar flux measurement technologies, or (2) the measurement of both the total efficiency and receiver thermal efficiency.

Solar flux measurement technologies which suit industrial needs do not need moving bars and are compatible with industrial-scale receivers, see also [8-14]. The solar field efficiency can be derived by

$$\eta_{\text{sol,field}} = P_{\text{in, ap}} / \sum_{i} \left(G_{\text{b}} A_{\text{net}} \rho_{s, \varphi} \xi \right)_{i}$$
(9)

with $P_{\rm in,ap}$ being the aperture input power measured by integrating the solar flux mapping results, $G_{\rm b}$ the direct normal irradiance, $A_{\rm net}$ the net heliostat aperture, $\rho_{\rm s,\phi}$ the solar mirror reflectance being multiplied with the mirror cleanliness ε of heliostat i.

A second alternative method is to measure the total efficiency (solar to thermal output) and the receiver thermal efficiency and dividing both to get the solar field efficiency.

$$\eta_{\text{sol,field}} = \eta_{\text{total}} / \eta_{\text{rec,th}}$$
(10)

The thermal output for the total efficiency can be estimated by the product of mass flow rate, specific heat capacity and increase between receiver input and output temperature of a fluid. The receiver thermal efficiency can be estimated by tests developed during the Solar Two Project [17] and its further developments [18,19].

4. Results and discussion

4.1. Sampling and influence of input parameters on the sample size

If the properties of the heliostats can be approximated by a normal distribution, either the level-1 approach or the level-2 approach can be chosen. As an example, for a field of 5000 heliostats with normally distributed characteristics, an estimated mean value for the tracking accuracy of $\mu_{\rm e}=1.0$ mrad and an estimated standard deviation of $\sigma_{\rm e}=0.2$ mrad are assumed. Permitting a relative error e^* of 3 %, the real mean value for tracking of all heliostats is in the range from 0.97 to 1.03 mrad. Desiring a 95 %-confidence (coverage factor k=2), the standard normal deviate z=1.96 is used. The number of heliostats n that must be characterized to be representative for the tracking deviation is 166. If permitting a relative error of 5 %, the output of Eqs. (7) or (8) is 61 heliostats, and with 10 % error it is 16 heliostats.

Table 2 shows the sample size for the different formulas for a relative error e^* of 5 %, and compares the values calculated by Eqs. (4), (7) and (8). It can be observed that the sample size calculated with Eq. (4), 'pull with putting back', does not depend on the heliostat field size and is

Table 2

Number of heliostats to be sampled for a relative error of $e^*=5$ % for an estimated mean value for tracking accuracy tracking $\mu_{\rm e}=1.0$ mrad, estimated standard deviation of $\sigma_{\rm e}=0.2$ mrad (coefficient of variation $V_{\rm e}=20$ %), with 95% of confidence (k=2; z=1.96), calculated with the Eqs. (4), (7) and (8). A relative error e^* of 5% means that the mean tracking error falls between 0.95 and 1.05 mrad with 95% confidence. These equations are valid under the assumption of a normal distribution.

Heliostat field size N_{pop}	Sample size n , Eq. (4)	Sample size <i>n</i> , Eq. (7)	Sample size <i>n</i> , Eq. (8)
100	62	39	39
500	62	55	55
1000	62	58	58
2000	62	60	60
5000	62	61	61
10,000	62	61	61

always largest. Equations (7), and Eq. (8) produce practically the same number of heliostats to be sampled. As the number of heliostats is limited, the authors recommend using either Eq. (7) or Eq. (8), both based on 'pull without putting back'.

Under the assumption of a normally distributed heliostat characteristics, Fig. 5 shows the sample size for the tracking deviation for three different error margins (left), and three different coefficients of variations (right), both as a function of the heliostat field size. It is noteworthy that the required sample size is nearly constant for solar plants with more than 2000 heliostats, regardless of the specific error margin used. However, a more stringent error margin requires a large increase in the number of essential measurements (samples). A higher expected coefficient of variation $V_{\rm e}$ also increases strongly the number of samples. Depending on the sensitivity of the performance parameter on the energy yield, a different error margin must be used for each parameter. Hence a different sample size n is calculated for each heliostat performance parameter. The procedure for selecting heliostat samples for measurement is performed in a fully randomized manner.

4.2. Process of estimation of the initial mean and standard deviation values

In the following, an example of a fictitious 50-MW plant with a total of 14,500 heliostats is used to discuss the process of estimation of the initial mean μ_e and standard deviation σ_e on the sampling for mirror reflectance, slope deviation and tracking accuracy. The estimated input parameters and the permitted relative error are listed in Table 3. In the case of mirror reflectance, assuming an estimated standard deviation σ_e of for example only 0.2 % means that we have to know previously that

200 Eq. (7), V =0.20, 95 % confidence 175 e*=3 % 150 -e*=5 % e*=10 % Sample size n 125 100 75 50 25 0 10² 10³ 10⁴ 10 Population N_{pop} (number of all heliostats in solar field)

there is no high variance in the delivered mirrors. Then, Eqs. (7) or (8) result in a sample size of 18 heliostats for reflectance, 82 for slope deviation and 62 for tracking accuracy. Fig. 6 shows the plant layout and the randomly selected heliostats for each parameter of Table 3.

The estimates have to be based on a critical engineering mind. If a very small coefficient of variation is used, like in the case of reflectance in the example of Table 3, it has to be checked beforehand that this is the case. Only then, a very small coefficient of variation of 0.002 is justified, resulting in the very small sample size of only 18 heliostats. On the other hand, if the evaluators suspect a wider variance of reflectance, the estimated standard deviation $\sigma_{\rm e}$ has to be increased, leading to a higher coefficient of variation $V_{\rm e}$ and hence larger sample size. An increase of $\sigma_{\rm e}=$ from 0.2 % to 0.8 % would increase the number of mirrors to be measured from 18 to 273.

The estimated values should be chosen conservatively to detect significant irregularities. The calculated sample size n should always be seen as a minimum. After sampling, the input parameters $\mu_{\rm e}$ and $\sigma_{\rm e}$ for the formulas may be compared with the observed ones ($\mu_{\rm s}, \, \sigma_{\rm s}$), and the sampling can be redone using these. This checks whether the sample size is sufficiently large. If not, more samples have to be taken.

The estimation of the mean and standard deviation values for sampling should be based on, amongst other: (1) qualification reports of the mirror production line with good coverage of sampling, (2) consideration of the different particularities of each construction site, like parts of a heliostat field may have been constructed in different phases and the first sector may be of worse quality, or there could have been several onsite assembly lines, each with different quality. (3) The usage of airborne image technologies should be considered to get deeper insight if there are clusters of worse quality.

However, the guideline does not solve the problem of making too optimistic estimations on the variance which might lead to the situation that heliostats with worse quality may be not detected at all. This is especially critical in the case of not normally distributed population where the application of the presented equations is not scientifically justified. In this sense, the procedure presented may not be the final one, and further guidance should be given in a final guideline. Additional safety factors on the resulting number of samples n could be applied for example, whenever there is little knowledge about the construction phases or drone screening measurements. The number of investigated heliostats may be increased until there is no significant change in the output.

The relative error e^* should be related to the sensitivity of the parameter on the energy yield. The higher the sensitivity, the lower the relative error e^* must be chosen. A scientific discussion, whether the sampling is sufficient and what is the significance of the uncertainty of

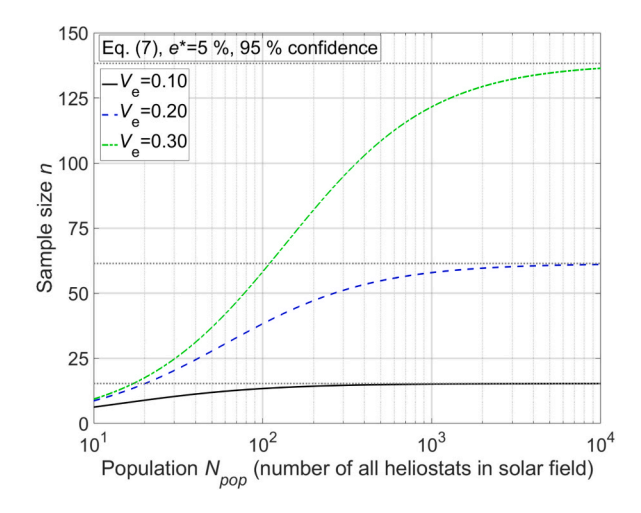


Fig. 5. Required quantity of heliostats n to be measured for representation of the heliostat field for 95 % confidence (z = 1.96) for different relative error margins e^* (coefficient of variation $V_e = 0.2$; left) and different coefficients of variations (relative error $e^* = 5$ %; right). The calculation is performed with Eq. (7).

Table 3 Estimated input parameters for Eqs. (7) or (8) and resulting heliostat sample size n for a fictitious field of $N_{pop} = 14500$ heliostats.

Parameter	Estimated mean (μ_e)	Estimated standard deviation (σ_e)	Estimated coefficient of variation (V_e)	Relative error (e*)	Resulting heliostat sample size (n)
Reflectance of clean mirror	94 %	0.2 %	0.002	0.1 %	18
$ ho_{s,\phi}$ Slope Deviation	1.3 mrad	0.3 mrad	0.23	5 %	82
SD _{2D,RMS} Tracking Accuracy Track _{2D,HCS,RMS}	0.5 mrad	0.2 mrad	0.40	10 %	62

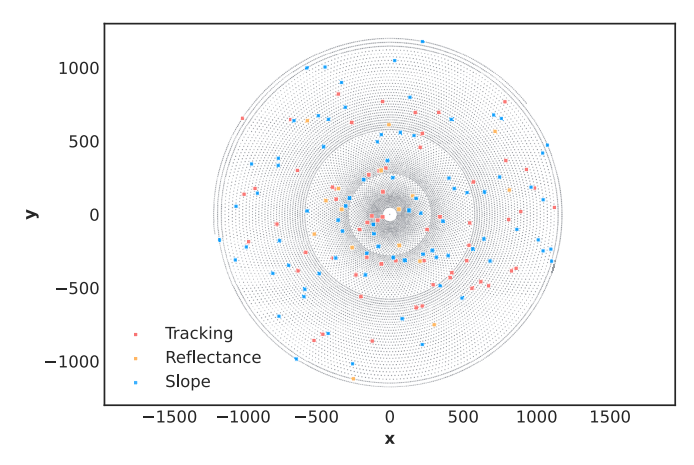


Fig. 6. Example of sampled heliostats which are marked with colors indicating the parameter to be measured: Tracking, reflectance and slope deviation; more details in Table 3.

each parameter on the energy yield is discussed in a separate article [50].

4.3. Comparison between approaches

In the level-1 approach, the guideline recommends evaluating the heliostat field quality by comparing distributions of heliostat parameters like tracking accuracy, reflectance and slope. Frequently, in a contractual agreement, the mean value and the standard deviation for each parameter are defined and compared. This procedure can be used for normally distributed populations which can be described by a mean value and standard deviation. It is easy to use and understand and less effort than defining a level-2 approach. However, local clusters of parameters of inferior quality are not represented correctly. The level-1 approach is not practical for not normally distributed populations.

In contrast, the level-2 approach can be used both for normally distributed and not normally distributed populations. Clusters of inferior quality can be represented in a more realistic way due to the possibility to represent the spatial occurrence of in a raytracing software. Of course, this is only feasible, if the sampling results are representative for the entire field, since the simulations of the level-2 approach can only give a result as good as the input. A cluster with higher tracking deviation for example has a lower effect on the spillage losses and receiver efficiency, if it is located closer to the tower. The energy yield calculated by the level-2 approach is a more relevant characteristic than mere heliostat properties. Agreeing on energy yield together with an aimpoint strategies or flux limits means that an EPC company may compensate one parameter with inferior quality with another with superior quality, or by simply using more heliostat units. Also, it is possible to include an aimpoint strategy in the contract. The level-2 approach is the more powerful, but more complex. It requires more work during the performance testing phase and needs more definitions in the contract, like definitions of a TMY, the raytracing program, aimpoint strategy, etc. The Heliodor project consortium recommends not to stop at level 1, but to continue with level 2.

Compared to the level-1 and level-2 approach based on statistical measurements and raytracing, the other approaches presented in section 3.4.3 in Eqs. (9) and (10) are not yet recommended at this development stage.

Solar flux measurement technologies without moving bar are in development and currently have still a high measurement uncertainty. A 1-sigma uncertainty of \pm 6.2 % for local solar flux density values is estimated by Offergeld [10] for a volumetric receiver with non-Lambertian reflection behavior, including a radiometer uncertainty of \pm 3.0 %. Raeder et al. [11] observe in two single tests deviations of the integrated solar flux with a reference measurement below 4.4 % for a tubular receiver with non-Lambertian reflection, excluding the uncertainty of the radiometer reading. Adding 3 % of radiometer uncertainty [5,6] results in an uncertainty below approximately \pm 5.3 %. Casanova et al. [14] report an uncertainty of the integrated flux of below \pm 5 %, but for receivers with Lambertian reflection behavior. When the uncertainty of these methods decreases, they probably may become a good method for acceptance in case of external receivers.

The second method to calculate heliostat field efficiency presented is the measurement of both the total efficiency and thermal receiver efficiency, see Eq. (10). The limiting factor is the determination of the receiver thermal efficiency in an industrial-scale solar plant. Its accuracy has still to be proved to be sufficient for acceptance testing. For these reasons, the Heliodor project consortium recommends using the level-2 approach based on statistical measurements and raytracing.

5. Experience from practical field test at the Juelich solar tower

A practical field test of the final acceptance step of the guideline was performed at the Solar Tower in Juelich, Germany. A simulated environment was set up with DLR as the owner, CSP Services as the measurement service provider and Synhelion as the heliostat manufacturer. The testing was performed in a subfield with 1001 heliostats where major components of the Juelich heliostat had been replaced. With a trained team and good preparation, the duration of the testing should take about one week.

5.1. Contractual agreement

The "contract" in this simulated environment defines both acceptable mean values and standard deviations (level-1), additionally to the yearly heliostat field efficiency, using an agreed TMY (level-2) with fixed sunshape and attenuation. It is assumed that the heliostat field cleanliness is 100 %. The validated raytracing software STRAL [51] was applied for both the contractually agreed and the calculated performance using the level-2 approach. For the exemplary testing of the guideline, the focus was restricted to four key performance parameters:

Net heliostat aperture $A_{\rm net}$ (level-1: $>8.178\pm0.007~{\rm m}^2$), solar-weighted reflectance of the clean mirror $\rho_{\rm s,\phi}$ ($>94.0\pm0.14$ %), 2D-slope deviation $SD_{\rm 2D,RMS}$ ($<1.5\pm0.3$ mrad), and 2D-tracking accuracy $Track_{\rm 2D,HCS,RMS}$ ($<2.0\pm0.2$ mrad). Some communication and safety parameters were tested also; however, this article only reports the subfield performance testing.

5.2. Sampling

As initial estimates for mean and standard deviation, the contractually agreed values have been taken. Table 4 shows the applied relative error e^* and the resulting heliostat sample size n for each parameter. The relative error should be related to the sensitivity of the parameter on the energy yield. The sensitivity is also printed in Table 4. More sensitive parameters generally require smaller relative errors. A small deviation in the net heliostat aperture and mirror reflectance has a direct effect on the energy yield, while the effect of slope and tracking deviations dependent on the design of the plant, mainly on the heliostat position in the field, its distance from the solar tower, the required solar concentrations in the receiver aperture, or the dimensions of the receiver aperture. More detailed studies will be given in a separate article [50].

A small estimated standard deviation σ_e is taken for the net heliostat aperture and clean mirror reflectance. This is because in the simulated environment of the project, it is assumed that test certificates from the mirror manufacturing lines are available (component pre-test) and that the batch numbers in the factory and on-site have been checked in the quality assurance plan during procurement and commissioning.

5.3. Measurement

5.3.1. Slope deviation

The slope deviation is measured using the installed QDec for heliostats deflectometry system [31] at the Juelich Solar Tower. This process is easily feasible within a single night due to its automation. A total of 27 randomly selected heliostats are measured. On-site concentrator manufacturing quality control with automated in-line measurements is an alternative to reduce acceptance test scope in the field. The possible impact of transport and final assembly at the destination in the solar field has to be considered and checked with a few measurements.

5.3.2. Clean mirror reflectance

Before measurement, the mirrors have been cleaned at the measurement locations. Then, the monochromatic reflectivity values $\rho_{\lambda,\phi}$ near the four heliostat corners are measured with a D&S reflectometer, with each location being measured twice. Subsequently, the mean reflectivity value is calculated for each heliostat. A total of ten randomly selected heliostats are measured.

The D&S handheld reflectometer measures the monochromatic

reflectivity $\rho_{\lambda,\phi}$ at a wavelength λ and an acceptance angle φ . However, for yield calculations, the solar-weighted reflectance $\rho_{s,\phi}$ is needed. For this reason, only the standard deviations of the individual reflectivity measurements are taken from the reflectometer readings. For the mean value of the solar-weighted reflectance $\rho_{s,\phi}$, before installation, randomly selected mirrors should be measured in a laboratory or during manufacturing with a spectrophotometer (component pre-test). The samples must be measured according to the SolarPACES reflectance guideline [52]. It is necessary to prove whether the same mirror batches are installed in the field. If there are any inconsistencies, further tests can be carried out.

5.3.3. Net heliostat aperture

The net heliostat aperture is measured using a tachymeter. Ten heliostats are sampled, with measurements taken at the corners of the four sub-mirror segments of each heliostat. The average edge length of the mirrors and based on that, the aperture area is calculated. As with reflectance, measurements taken on samples in the laboratory can be used (component pre-test).

5.3.4. Tracking accuracy

The tracking accuracy is evaluated using the installed beam characterization system. A total of 24 heliostats are characterized. The position of the focal spot of the heliostat on a white target is measured by a camera. Due to the fact that we need to characterize the tracking accuracy for several heliostats, the procedure deviates from the one described in the SolarPACES Guideline for Heliostat Performance Testing. Instead of continuously focusing one heliostat over several hours, each heliostat is measured in several homogeneously distributed time series of a few minutes over a day. Three to five time series should be taken for each heliostat. In each time slot (e.g. 1 h), a whole group of heliostats is measured, and then the whole group is measured again in the next time slot, and so on.

5.4. Results and discussion

Fig. 7 shows the measured distribution functions of the results for slope deviation, clean mirror reflectance, net heliostat aperture, and 2D tracking accuracy. The measured mean values of the samples μ_s and the expected mean values μ_e . are shown by vertical lines. The figure includes a box plot comparing the measured standard deviation σ_s with the expected standard observation σ_e . Table 5 shows a comparison of the contractually specified with the measured values.

5.4.1. Slope deviation

For slope deviation, the measured mean value and standard deviation are slightly lower than the estimated ones. Hence, the observed coefficient of variation V_s is slightly lower as expected. There is no

Table 4 Minimum number n of heliostats to be sampled with estimated statistical input parameters, relative error margin e^* and expected range for the mean value in the Juelich heliostat subfield (1001 heliostats). A 95 % confidence interval (k = 2; z = 1.96) is assumed.

Parameter	Estimated mean and standard deviation $(\mu_e \pm \sigma_e)$	Estimated coefficient of variation (V _e)	Relative error (e*) Interval	Expected range of μ (95 % confidence)	Sensitivity of the parameter on energy yield	Resulting heliostat sample size (n)
Slope Deviation $SD_{\mathrm{2D,RMS}}$	$1.5 \pm 0.3 \; \text{mrad}$	0.20	7.5 %	[1.4; 1.6] mrad	medium	27
Reflectance of clean mirror	94.0 \pm 0.14 %	0.0015	0.1 %	[93.9; 94.1] %	high	10
$ ho_{ extsf{s}, \phi}$ Net heliostat aperture $A_{ extnormal{net}}$	$8.178 \pm 0.007 \text{ m}^2$	0.0008	0.05 %	[8.174; 8.182] m ²	high	10
Tracking Accuracy <i>Track</i> _{2D,HCS,RMS}	$2.0 \pm 0.2 \text{ mrad}$	0.10	4 %	[1.9; 2.1] mrad	medium	24

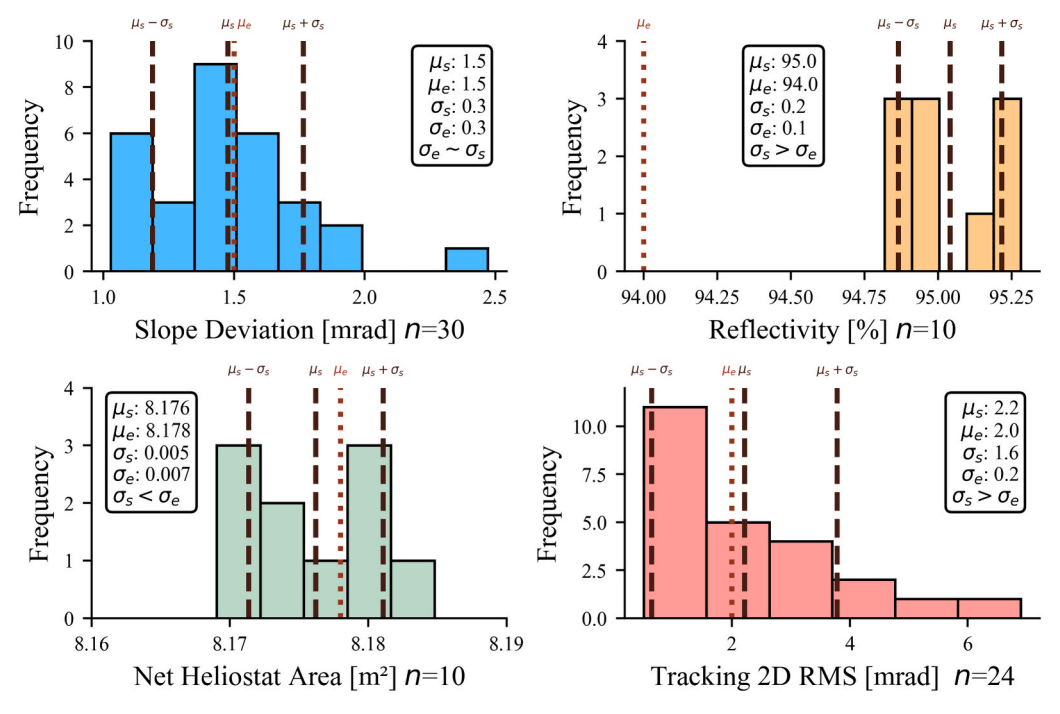


Fig. 7. Measured distribution functions of the sampled heliostats for slope deviation, clean mirror reflectance/reflectivity, net heliostat aperture, and 2D tracking accuracy (RMS).

Table 5

Comparison of the contractually specified values with the measurement campaign results for the four examined parameters in the investigated subfield (1001 heliostats). The contractually agreed values also served as estimations for the first sampling. The last column shows the sampled coefficient of variation and compares the value to the estimated one.

Parameter	Contractually a Estimated mean (μ_e)	greed values Estimated standard deviation (σ_e)	Estimated coefficient of variation (V_e)	Measured values Sampled mean (μ_s)	Sampled standard deviation (σ_s)	Sampled coefficient of variation (V_s)
Slope	1.5 mrad	± 0.3 mrad	0.20	1.5 mrad	± 0.3 mrad	0.20 (similar)
Deviation $SD_{ m 2D,RMS}$						
Reflectance / Reflectivity of clean mirror	$\rho_{\rm s,\phi}=94.0~\%$	$\pm 0.14~\%$	0.0015	$\rho_{\lambda,\phi} = 95.0 \%$	$\pm 0.18~\%$	0.0019 (1.3x higher)
Net heliostat aperture A_{net}	8.178 m ²	$\pm 0.007~\text{m}^2$	0.0008	8.176 m ²	$\pm 0.005~\text{m}^2$	0.0006 (0.7x lower)
Tracking Acc. Track _{2D,HCS,RMS} Subfield	2.0 mrad	$\pm 0.2 \; \text{mrad}$	0.10	2.2 mrad	$\pm 1.6 \; mrad$	0.73 (7x higher)
Orange cluster				2.8 mrad	± 1.9 mrad	0.67 (7x higher)
Red cluster				1.7 mrad	± 0.5 mrad	0.30 (3x higher)
Blue cluster				1.7 mrad	± 1.8 mrad	1.07 (11x higher)

indication of the need for additional sampling. The distribution function follows the expected Weibull-type distribution.

5.4.2. Clean mirror reflectance

Regarding reflectivity, the measured standard deviation is about 26 % larger than the estimated. And, the mean value of the monochromatic reflectivity $\rho_{\lambda,\phi}$ measured by the reflectometer is 1 percent point higher than the estimated solar-weighted reflectance $\rho_{s,\phi}$, although both values are not directly comparable. The observed coefficient of variation V_s is higher than the estimated V_e . Consequently, three additional samples would have been necessary to achieve statistically significant results. However, due to time constraints, this additional measurement has been omitted in the project. Increasing the sample size probably would have made the normal distribution of reflectance more apparent. The solar-weighted reflectance $\rho_{s,\phi}$, not measurable by a field instrument, is needed for level-2 calculations. In the simulated environment of the project, it is assumed that the qualifying company proves that the a solar-weighted reflectance $\rho_{s,\phi}$ of 94 % has been observed by pre-

component testing beforehand. In other words, it is assumed that the measured mean solar-weighted reflectance is as contractually agreed.

5.4.3. Net heliostat aperture

For the net aperture area, the standard deviation of the sample is below the estimated value, and the sampled mean aligned well with the estimate. Thus, the selected sample size is sufficient.

5.4.4. Tracking accuracy

While the measured, mean tracking deviation is about 10 % higher than the expected mean values the standard deviation is almost a factor eight higher than anticipated. This increased variability suggests that some heliostats are quite good, but others require additional calibration points to achieve the desired accuracy.

Fig. 8 shows the investigated heliostat subfield. The 24 sampled heliostats for the tracking accuracy are shown as colored rectangles. The rectangle size is a measure of the tracking deviation. A cluster analysis algorithm run on the sampled data successfully identified a group of

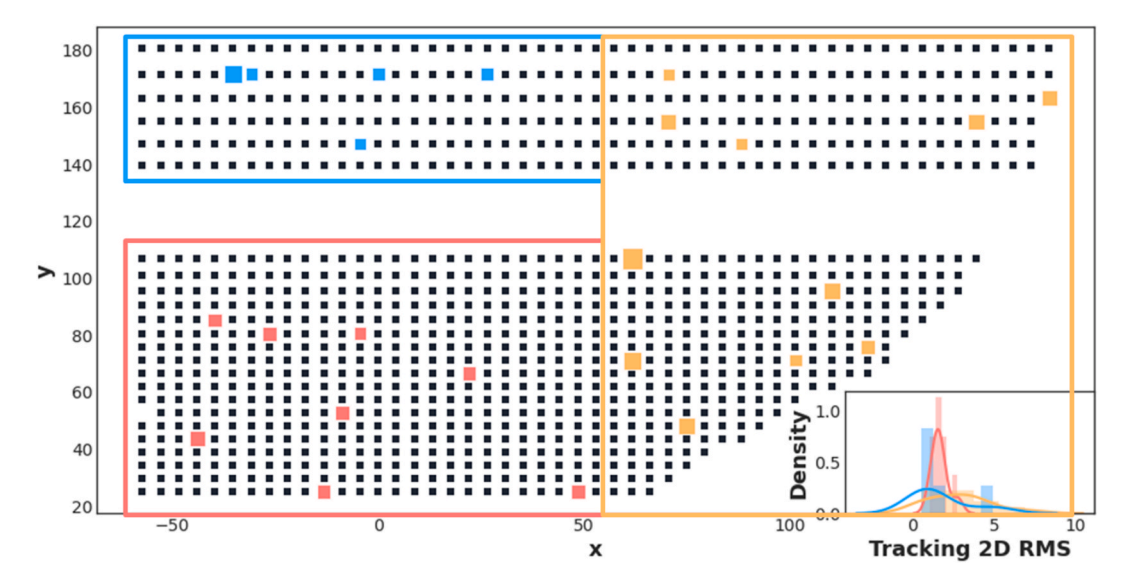


Fig. 8. Heliostat subfield to which the acceptance guideline is applied. The size of each rectangle represents the tracking accuracy level. The clusters are delineated by rectangles. Additionally, the distribution functions in the lower-right panel illustrate the characteristics of each cluster.

heliostats exhibiting poorer aiming performance compared to other areas. This group is displayed in the orange frame and the measured values in the lower part of Table 5. Upon investigation, the heliostats had been recently refurbished and had not yet accumulated sufficient calibration points for accurate sun tracking. Under commercial conditions, these heliostats would likely not have passed the readiness for acceptance test or the provisional acceptance test, and the final acceptance test would have been postponed in order to totally calibrate the field to pass the readiness for final acceptance testing.

If the test had continued with the underlying mix of well and moderately calibrated heliostats, the number of samples would have grown significantly. In the orange cluster with 377 heliostats, for example, the found high mean value $\mu_{\rm S}$ of approximately 2.8 mrad and high standard deviation $\sigma_{\rm S}$ of 1.9 mrad increases the observed coefficient of variation $V_{\rm S}$ over the expected one in Table 4. This would require an additional 270 tracking measurements in this cluster to achieve statistical significance.

In contrast to the orange cluster, the red and blue ones show in average well-calibrated heliostats. However, both clusters have a higher variance in calibration quality than anticipated. Especially the blue cluster contains some few heliostats with very poor aiming quality, which increases the variance in this group to a value almost as high as in the orange cluster. This special situation of a not totally calibrated field with high variance in aimpoint quality –7 times higher than estimated—may occur in reality, but usually the acceptance test is interrupted to terminate the calibration. If not, a lot of additional heliostats have to be measured and the field may not pass the acceptance test.

The findings about the quality of the clusters have been confirmed by the heliostat field managers. Heliostats in the orange cluster have been recently installed and therefore have not had enough calibration points for a proper sun tracking. Certainly, in a commercial setting, these heliostats would not have passed the "readiness for acceptance" test and the final acceptance test would have been postponed. The cluster analysis has demonstrated the utility of the method in extracting meaningful information and identifying specific field regions that require revision, recalibration, or more detailed sampling.

In the simulated environment of the project, the consortium decided to continue the acceptance test as a provisional acceptance test, but, for time reasons, without resampling and measurement of additional heliostats, which is not conform to the proposed methodology.

5.4.5. Level-1 approach

Comparing the measured and contractually agreed mean values and standard deviations in Table 5, the EPC contractor fulfills the specifications for slope deviation, reflectance, and heliostat aperture, but not for tracking accuracy. Hence, the result of the acceptance test is "failed".

5.4.6. Level-2 approach

In level-2, the DLR raytracing tool STRAL is used with the defined TMY, sunshape and attenuation to assess the monthly and annual heliostat field efficiency, see Fig. 9. For each cluster, the sampled values were extrapolated using KDE and assigned to the not measured heliostats

The simulation indicate that the investigated subfield has an approximately 0.2 % lower yearly efficiency than agreed in the contract caused by the low tracking accuracy of some heliostats, especially in the orange cluster. Hence, the result of the acceptance test for performance is "failed".

Despite the notably high standard deviation in the tracking error, the aggregate impact on system performance was limited.

5.5. Lessons learned

In general, the acceptance procedure using the level-2 approach went without encountering major problems. The project consortium learned the following during the execution:

- It is of major importance to correctly choose estimated mean and standard deviation values, based on a critical engineering mind, considering results of component pre-tests or on-site quality assurance equipment, if available.
- Knowledge about the heliostat field production order and manufacturing process helps to confirm the results of a cluster analysis.
- If after a cluster analysis, there is a high standard deviation in all the sectors, a cluster analysis might not help to reduce the total amount of heliostats to be characterized. If different sectors have different qualities or standard deviation, then clustering is helpful to reduce the number.
- The mean value for solar-weighted mirror reflectance should be measured with a spectrophotometer preferably before installation in the laboratory (component pre-testing). Post-cleaning reflectivity

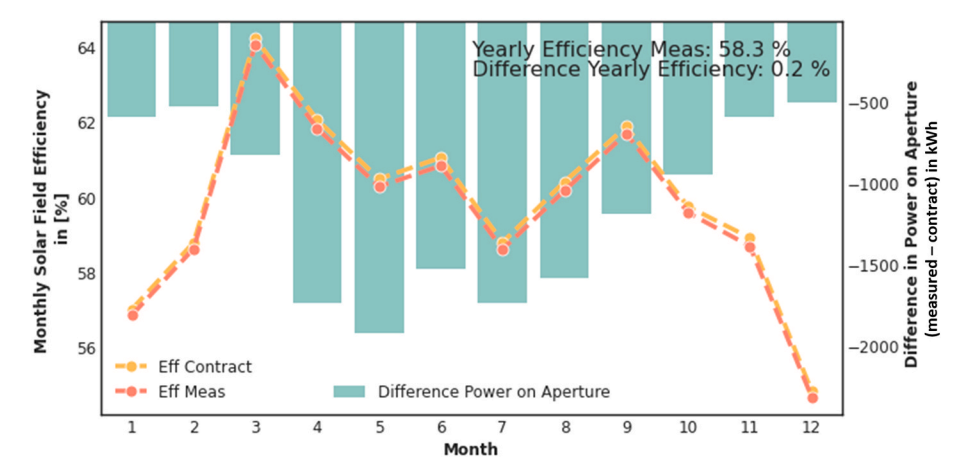


Fig. 9. Comparison of the simulated monthly solar field efficiency based on contractually agreed values (Eff contract) and the measurement campaign results (Eff meas). The bars indicate the monthly difference in collected energy in the receiver aperture plane between measured and contractually agreed values.

variations can be verified in the field using a standard handheld reflectometer.

- The test for tracking accuracy deviates from the test described in the SolarPACES Guideline for Heliostat Performance Testing [45] in the sense, that one heliostat is tested in three to five time intervals over the day during a few minutes only, hence allowing the characterization of more heliostats during a day.
- The acceptance procedure identifies specific field regions which require revision, recalibration, or a more detailed sampling.
- The level-2 approach, although being more work, showed its benefits compared to the level-1 approach. It can compensate for poor performance in one parameter with better improved performance in another.

Overall, the developed guideline proves to be an efficient tool for conducting heliostat field acceptance tests. It provides the necessary decision-making flexibility regarding the choice of measurement methods for each parameter and allows for adaptability in determining the required accuracy. Additionally, the guideline offers actionable recommendations, such as interrupting the acceptance process for further technical revision.

6. Conclusion and Outlook

The Heliostat Field Performance Testing Guideline addresses the challenge of objectively and practically assessing the performance of large-scale heliostat fields and serves as a basis for performance acceptance testing in an industrial context. The guideline is designed to increase confidence among stakeholders involved in commercial CSP central receiver projects. By providing generally accepted protocols, it establishes a standardized framework for meeting contractual obligations, ultimately increasing the reliability of commercial projects.

The Heliostat Field Performance Testing Guideline complements the SolarPACES Guideline for Heliostat Performance Testing [45], which defines parameters and respective measurement techniques of individual heliostats.

The level-1 approach of the Heliostat Field Performance Testing Guideline selects a statistically relevant number of heliostat samples and compares the heliostat characteristics (e.g. slope deviation, tracking deviation, etc.) with contractually defined values. The recommended level-2 approach uses level-1 data to extend the measurement results to unmeasured heliostats and performs a raytracing yield simulation with energy yield outputs and solar field efficiency calculations. The guideline also includes additional material, such as a sample acceptance procedure for a fictitious power plant and a sample contract between the heliostat field manufacturer and the owner.

Experience from practical level-2 field tests at the Juelich Solar Tower demonstrate the viability of the approach provided the sampling is representative. It is confirmed that the geometric performance parameters, like slope deviation and tracking accuracy have a high sensitivity on the results. It is also shown that the cluster analysis algorithm can successfully detect regions of heliostats with poorer aimpointing.

The lessons learned are included into the final, national guideline document which will be distributed for international review to the SolarPACES Task III Heliostat Working Group. Further scientific publications on the methods are planned.

Competing interests.

The authors declare that they have no competing interests.

Declaration of Generative AI and AI-assisted technologies in the writing process

Statement: During the preparation of this work the authors used "DEEPL Write" in some paragraphs to improve readability and language for some sections of the text. After using this tool/service, the authors reviewed and edited the content as needed and take full responsibility for the content of the publication.

CRediT authorship contribution statement

Marc Röger: Writing - original draft, Supervision, Project administration, Methodology, Funding acquisition, Conceptualization. Tim Schlichting: Writing - review & editing, Visualization, Validation, Software, Methodology, Investigation, Formal analysis, Conceptualization. Jakob Herrmann: Writing - review & editing, Project administration, Methodology, Funding acquisition. Christoph Happich: Writing - review & editing, Validation, Project administration, Methodology, Investigation, Formal analysis. Daniel Nieffer: Writing - review & editing, Project administration, Methodology, Funding acquisition. Gerhard Weinrebe: Writing - review & editing, Supervision, Project administration, Methodology, Funding acquisition. Patrick Hilger: Writing – review & editing, Validation, Project administration, Methodology, Funding acquisition. **Ansgar Macke:** Writing – review & editing, Validation, Investigation, Formal analysis. Kristina Blume: Writing - review & editing, Validation, Methodology, Investigation, Formal analysis. Fabian Gross: Writing - review & editing, Methodology.

Funding

Financial support from the German Federal Ministry for Economic Affairs and Energy (HELIODOR, contract 0324310) is gratefully

acknowledged. The SFERA-III project (Grant Agreement 823802, European Union's Horizon2020 Research and Innovation Programme) supported the guideline by funding international standardization activities.

Acknowledgement

The authors gratefully acknowledge the German Federal Ministry for Economic Affairs and Climate Action and the European Union for funding. The authors also thank the DLR colleagues at the Juelich Solar Tower for providing access to the solar field.

References

- E. Thalhammer, "Heliostat Beam Characterization System—Update," I.S.A. Reprint 79-692 (1979). ISA-79 National Conference and Exhibit. Chicago. Illinois.
- [2] D. King, D. Arvizu, Heliostat characterization at the central receiver test facility,
 J. Sol. Energy Eng. 103 (2) (1981) 82–88, https://doi.org/10.1115/1.3266229.
- [3] A. Kröger-Vodde, A., Holländer, A., 1999. CCD flux measurement system PROHERMES. J. Phys. IV 9 (PR3) Pr3–649, DOI: https://doi.org/10.1051/jp4 19993103
- [4] J. Ballestrín, R. Monterreal, Hybrid Heat Flux Measurement System for Solar Central Receiver Evaluation,", Energy 29 (5–6) (2004) 915–924, https://doi.org/ 10.1016/S0360-5442(03)00196-8.
- [5] S. Ulmer, Messung der Strahlungsflussdichte-Verteilung von punktkonzentrierenden solarthermischen Kraftwerken, PhD thesis, University of Stuttgart, Aug 2003.
- [6] S. Ulmer, E. Lüpfert, M. Pfänder, R. Buck, Calibration corrections of solar tower flux density measurements, Energy 29 (2004) 925–933, https://doi.org/10.1016/ S0360-5442(03)00197-X.
- [7] M. Ebert, D. Benitez, M. Röger, R. Korzynietz, J.A. Brioso, Efficiency determination of tubular solar receivers in central receiver systems, Sol. Energy 139 (2016) 179–189, https://doi.org/10.1016/j.solener.2016.08.047.
- [8] M. Röger, P. Herrmann, S. Ulmer, M. Ebert, C. Prahl, Techniques to measure solar flux density distribution on large-scale receivers, J. Sol. Energy Eng. 136 (3) (2014) 031013, https://doi.org/10.1115/1.40272616.
- [9] M. Offergeld, M. Röger, H. Stadler und P. Gorzalka, Flux density measurement for industrial-scale solar power towers using the reflection off the absorber, AIP Conference Proceedings 2126, 110002 (2019), SolarPACES, Casablanca, 2018, DOI: https://doi.org/10.1063/1.5117617.
- [10] M. Offergeld, Flux density measurement using the reflection at external receivers of industrial scale solar tower plants, Dissertation, RWTH Aachen University (2023), https://doi.org/10.18154/RWTH-2024-08822.
- [11] C. Raeder, M. Offergeld, M. Röger, A. Lademann, K. Zöller, M. Glinka, J. Escamilla, A. Kämpgen, Proof of Concept: Real-time flux density monitoring system on external tube receivers for optimized solar field operation, AIP Conf. Proc. 2815 (2023) 080008, https://doi.org/10.1063/5.0148725.
- [12] C.K. Ho, S.S. Khalsa, A Photographic Flux Mapping Method for Concentrating Solar Collectors and Receivers, J. Sol. Energy Eng. Nov 2012, 134(4): 041004 (8 pages), DOI: https://doi.org/10.1115/1.4006892.
- [13] J. Ballestrín, M. Casanova, R. Monterreal, J. Fernández-Reche, E. Setien, J. Rodríguez, J. Galindo, F.J. Barbero, F.J. Batlles, Simplifying the measurement of high solar irradiance on receivers, Application to Solar Tower Plants, Renewable Energy 138 (2019) 551–561, https://doi.org/10.1016/j.renene.2019.01.131.
- [14] M. Casanova, J. Ballestrín, R. Monterreal, J. Fernández-Reche, R. Enrique, A. Ávila-Marín, Improvements in the measurement of high solar irradiance on a 300 kWth volumetric receiver, Renew. Energy 201 (2022) 441–449, https://doi.org/10.1016/j.renene.2022.10.080.
- [15] D. Kearny, Utility-Scale Power Tower Solar Systems: Performance Acceptance Test Guidelines, NREL Report NREL/SR-5500-57272, March 2013, DOI: https://doi. org/10.2172/1069189.
- [16] D. Kearny, Utility-Scale Power Tower Solar Systems: Performance Acceptance Test guidelines, Energy Procedia 49 (2014) 1784–1791, https://doi.org/10.1016/j. egypro.2014.03.189.
- [17] J. Pacheco, et al., Final Test and Evaluation results from the Solar two Project, SAND2002-0120, Albuquerque, NM (2002), https://doi.org/10.2172/793226.
- [18] M. Fernández-Torrijos, C. Frantz, J. Stengler, M. Röger, T. Schlichting, R. Buck, Experimental Methods for measuring the Efficiency of a Molten Salt Central Receiver, SolarPACES Conference Proceedings, 1, Albuquerque, NM, US (2024), https://doi.org/10.52825/solarpaces.y1i.715.
- [19] G. Xiao, J. Zeng, J. Nie, A practical method to evaluate the thermal efficiency of solar molten salt receivers, Appl. Therm. Eng. 190 (2021) 116787, https://doi.org/ 10.1016/j.applthermaleng.2021.116787.
- [20] G. Zhu, C. Augustine, R. Mitchell, M. Muller, P. Kurup, A. Zolan, S. Yellapantula, R. Brost, K. Armijo, J. Sment, R. Schaller, M. Gordon, M. Collins, J. Coventry, J. Pye, M. Cholette, G. Picotti, M. Arjomandi, M. Emes, D. Potter, M. Rae, HelioCon: a roadmap for advanced heliostat technologies for concentrating solar power, Sol. Energy 264 (2023) 111917, https://doi.org/10.1016/j.solener.2023.111917
- [21] A. Peña-Lapuente, M. Röger, J. Fernández, J. Pye, M. Collins, M. Blanco, J. Gonzalez-Aguilar, G. Zhu, C. Villasante, K.M. Armijo, S. Ulmer, G. Bern, P. Gauche, J. Fernando Gallego, J.M. Blázquez, SolarPACES Task III project: Analyze Heliostat Field: Results of methodologies comparison, gaps to be filled and next steps to

- further improve the solar central receiver technology, SolarPACES Conference Proceedings, 2, 2024, DOI: https://doi.org/10.52825/solarpaces.v2i.903.
- [22] N.C. Cruz, R. Monterreal, J.L. Redondo, J. Fernandez-Reche, R. Enrique, P. M. Ortigosa, Optical characterization of heliostat facets based on computational optimization, Sol. Energy 248 (2022) 1–15, https://doi.org/10.1016/j.solener.2022.10.043.
- [23] J. Lewen, M. Pargmann, M. Cherti, J. Jitsev, R. Pitz-Paal, D. Maldonado Quinto, Inverse deep learning raytracing for heliostat surface prediction, Solar Energy 289 (2025) 113312, https://doi.org/10.1016/j.solener.2025.113312.
- [24] A. Martínez-Hernández, R. Conceição, C.A. Asselineau, M. Romero, J. González-Aguilar, Advanced surface reconstruction method for solar reflective concentrators by flux mapping, Sol. Energy 266 (2023) 112162, https://doi.org/10.1016/j.solener.2023.112162.
- [25] A. Peña-Lapuente, S. Escorza, A. Mutuberria, M. Sánchez, J. García-Barberena, C. Heras, A. Villafranca, Novel scanner-based methodology for a fast and complete high quality characterization of all solar field heliostats, their facets, and corresponding reflected beams, Proc. SPIE 12671, advances in Solar Energy: Heliostat Systems Design, Implementation, and Operation (2023), https://doi.org/ 10.1117/12.2677246
- [26] C. Andraka, S. Sadlon, B. Myer, K. Trapeznijov, C. Liebner, Rapid Reflective Facet Characterization using Fringe Reflection Techniques, Solar Energy Engineering 136 (2014), https://doi.org/10.1115/1.4024250.
- [27] R.C. Brost, B. Smith, F. Brimigion, B. Bean, A. Evans, SOFAST 2.0: Open-Source Deflectometry for CSP, SolarPACES 2024, 30th Intern. Conf. on Solar Power & Chemical Energy Systems, Rome, Oct 8–11,2024, Italy.
- [28] R.C. Brost, B. Smith, F. Brimigion, Agile Deflectometry, SolarPACES, Conference Proceedings 1 (2023), https://doi.org/10.52825/solarpaces.v1i.709.
- [29] B. Smith, R.C. Brost, Robust Deflectometry, SolarPACES, Conference Proceedings 2 (2024), https://doi.org/10.52825/solarpaces.v2i.756.
- [30] T. März, C. Prahl, S. Ulmer, S. Wilbert, C. Weber, Validation of Two Optical Measurement Methods for the Qualification of the Shape Accuracy of Mirror Panels for Concentrating Solar Systems, J. Sol. Energy Eng. 133 (2011), 031022 (7 pages), DOI: https://doi.org/10.1115/1.4004240.
- [31] S. Ulmer, T. März, C. Prahl, W. Reinalter, B. Belhomme, Automated high resolution measurement of heliostat slope errors, Sol. Energy 85 (2011) 685–687, https://doi. org/10.1016/j.solener.2010.01.010.
- [32] CSP Services. QDec system. https://www.cspservices.de/wp-content/uploads/ CSPS-QDec.pdf (retrieved 02.05.25).
- [33] J. Burke, W. Li, A. Heimsath, C. von Kopylow, R.B. Bergmann, Qualifying parabolic mirrors with deflectometry, J. Eur. Opt. Soc.-Rapid Publ. 8 (2013) 13014, https://doi.org/10.2971/jeos.2013.13014.
- [34] D. Kesseli, M. Keshiro, R. Mitchell, G. Zhu, A New Reflected Target Optical Assessment System: stage 1 Development results, SolarPACES Conference Proceedings 1 (2023), https://doi.org/10.52825/solarpaces.v1i.618.
- [35] D. Kesseli, D. Tsvankin, F. Tucker, R. Mitchell, D. Milo, G. Zhu, Improvements in Optical Surface Measurement Using Reflected Computer Vision Targets, SolarPACES 2024, 30th Intern. Conf. on Solar Power & Chemical Energy Systems, Rome. Oct 8–11.2024. Italy.
- [36] R. Mitchell, G. Zhu, A non-intrusive optical (NIO) approach to characterize heliostats in utility-scale power tower plants, Sol. Energy 209 (2020) 431–445, https://doi.org/10.1016/j.solener.2020.09.004.
- [37] T. Farrell, K. Guye, R. Mitchell, G. Zhu, A non-intrusive optical approach to characterize heliostats in utility-scale power tower plants: Flight path generation/ optimization of unmanned aerial systems, Sol. Energy 225 (2021) 784–801, https://doi.org/10.1016/j.solener.2021.07.070.
- [38] W. Jessen, M. Röger, C. Prahl, R. Pitz-Paal, A Two-Stage Method for measuring the Heliostat Offset, AIP Conf. Proc. 2445 (2022) 070005, https://doi.org/10.1063/ 5.0087036
- [39] J. Krauth, C. Happich, N. Algner, R. Broda, A. Kämpgen, A. Schnerring, S. Ulmer, M. Röger, HelioPoint – A Fast Airborne Calibration Method for Heliostat Fields, J. Sol. Energy Eng. 146(6), 2024, DOI: https://doi.org/10.1115/1.4065868.
- [40] R. Brost, P. Apostolopoulos, D. Small, D. Novick, N. Jackson, M. Mann, E. Tsiropoulou, (2021). High-Speed In Situ Optical Scanning of Heliostat Fields. SolarPACES 2021, https://www.osti.gov/servlets/purl/1888689 (retrieved 02.05.2025).
- [41] K. Pottler, E. Lüpfert, G.H.G. Johnston, M.R. Shortis, Photogrammetry: a powerful tool for geometric analysis of solar concentrators and their components, J. Sol. Energy Eng. 127 (1) (2005) 94–101, https://doi.org/10.1115/1.1824109.
- [42] M. Röger, C. Prahl, S. Ulmer, Heliostat shape and orientation by edge detection, J. Sol. Energy Eng. 132 (2) (2010) 021002, https://doi.org/10.1115/1.4001400.
- [43] K. Milidonis, D. Abate, M.J. Blanco, Heliostat geometrical characterization by UAV-assisted, close-range photogrammetry, Sol. Energy 280 (2024) 112849, https://doi.org/10.1016/j.solener.2024.112849.
- https://doi.org/10.1016/j.solener.2024.112849.

 [44] M. Röger, T. Schlichting, K. Blume, D. Nieffer, G. Weinrebe, C. Happich, A. Macke, J. Herrmann, T. Doerbeck, P. Hilger, HELIODOR Abnahmeverfahren für Heliostatfelder, Final Report (in German) (2022), https://doi.org/10.2314/KXP: 1891017411.
- [45] M. Röger, et al., SolarPACES Guideline for Heliostat Performance Testing, Version 1.0, in: SolarPACES, Task III, 2022, https://doi.org/10.5281/zenodo.15365474. https://www.solarpaces.org/.
- [46] M. Röger, K. Blume, T. Schlichting, M. Collins, "Status Update of the SolarPACES Heliostat Testing Activities," SolarPACES 2020, Online Event (Paper), AIP Conf. Proc. 2445 (2022) 070010, https://doi.org/10.1063/5.0087037.
- [47] M. Röger, T. Schlichting, K. Blume, Guidelines for heliostat testing, Proc. SPIE 12671, Advances in Solar Energy: Heliostat Systems Design, Implementation, and Operation, 1267106 (4 October 2023), https://dx.doi.org/10.1117/12.2682675.

- [48] D. Nieffer, T. Effertz, A. Macke, M. Röger, G. Weinrebe, S. Ulmer, "Heliostat Testing According to SolarPACES Task III Guideline," AIP Conference Proceedings 2126, (2019), 030039, SolarPACES, Casablanca, 2018, DOI: https://doi.org/ 10.1063/1.5117551.
- [49] [Lippe] Von der Lippe, Peter, Wie groß muss meine Stichprobe sein, damit sie repräsentativ ist? Contribution to Faculty Economics of the University Duisburg-Essen, No. 187, Febr. 2011, https://www.wiwi.uni-due.de/fileadmin/fileupload/ WIWI/Forschung/IBES_Diskussionbeitraege/187_Diskussionsbeitrag.pdf (retrieved 02.05.2025).
- [50] T. Schlichting, M. Röger, R. Pitz-Paal, Statistical Framework for Acceptance and Performance Evaluation of Heliostat Fields, to be sent to Solar Energy for review (2025)
- [51] B. Belhomme, R. Pitz-Paal, P. Schwarzbözl, S. Ulmer, New fast ray tracing tool for high-precision simulation of heliostat fields, J. Sol. Energy Eng. 131 (3) (2009) 031002, https://doi.org/10.1115/1.3139139.
- [52] A. Fernández-García, F. Sutter, M. Montecchi, F. Sallaberry, A. Heimsath, C. Heras, E. Le Baron, A. Soum-Glaude, Parameters and method to evaluate the reflectance properties of reflector materials for concentrating solar power technology under laboratory conditions – Official Reflectance Guideline Version 3.1, April, 2020, https://www.solarpaces.org/task-iii-solar-technology-and-advanced-applications/ optical-properties-working-group/ (retrieved 02.05.25).